

## Comparison of methods for obtaining a hydroxyapatite and zinc oxide composite (HAp/ZnO)

### Comparación de métodos para la obtención de un compósito de hidroxiapatita y óxido de zinc (HAp/ZnO)

Dávalos-Rosas, Vivian Guadalupe<sup>a</sup>, García-González, Nidia\*<sup>b</sup>, Enríquez-Pérez, Ma. de los Ángeles<sup>c</sup> and Castrejón-Sánchez, Víctor Hugo<sup>d</sup>

<sup>a</sup> ROR Tecnológico de Estudios Superiores de Jocotitlán • LBH-2781-2024 • 0009-0003-5938-1063 • 2038349

<sup>b</sup> ROR Tecnológico de Estudios Superiores de Jocotitlán • LBH-2754-2024 • 0000-0001-8968-1233 • 240047

<sup>c</sup> ROR Tecnológico de Estudios Superiores de Jocotitlán • H-9399-2018 • 0000-0002-2280-0661

<sup>d</sup> ROR Tecnológico de Estudios Superiores de Jocotitlán • C-9077-2015 • 0000-0002-0112-5388 • 235470

#### CONAHCYT classification:

Area: Physics-Mathematics and Earth Sciences

Field: Physics

Discipline: Physics of the solid state

Subdiscipline: Composite materials

doi: <https://doi.org/10.35429/JOTI.2024.8.21.1.12>

#### Article History:

Received: January 13, 2024

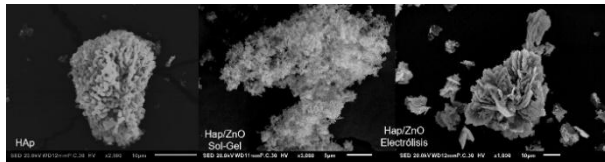
Accepted: December 31, 2024



\* ✉ [nidia.gonzalez@tesjo.edu.mx]

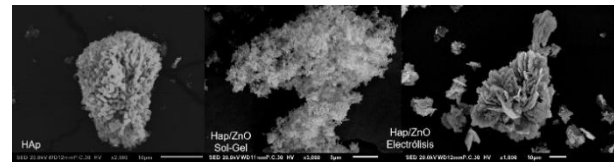
#### Abstract

In this work, the synthesis of a composite material based on hydroxyapatite (HAp) and zinc oxide (ZnO) is reported. Two types of synthesis were evaluated, in order to know which of them allows to obtain a homogeneous composite material of HAp and ZnO, since making a composite material implies that two or more compounds must be integrated and do not separate; the HAp will be obtained from eggshell residue, ZnO will be synthesized by Sol-Gel and electrolysis; in the ZnO obtention, the previously synthesized HAp was incorporated and it is followed by a thermal treatment obtain the oxide. To evaluate the incorporation of ZnO with hydroxyapatite, Scanning Electron Microscopy, Elemental Analysis and Mapping by Energy Dispersive Spectrometry, Infrared Spectroscopy Analysis and X-ray Diffraction were performed. These two synthesis methods are aiming to obtain a homogeneous material, establishing a methodology to produce the material composite, as well as improve the photocatalytic properties.



#### Resumen

Este trabajo aborda la síntesis de un material compuesto con hidroxiapatita (HAp) y óxido de zinc (ZnO), se evaluarán dos tipos de síntesis para conocer cuál de ellas permite obtener un compósito homogéneo de HAp y ZnO, ya que el hacer un compósito implica que dos compuestos se integren sin separarse; la HAp se obtendrá del cascarón de huevo (residuo), el ZnO se obtendrá por síntesis Sol-Gel y electrólisis. Al realizar la síntesis del ZnO se incorporó la HAp previamente sintetizada y se dio el tratamiento térmico para obtener el óxido. Para evaluar la incorporación de ZnO en la HAp se realizó Microscopía Electrónica de Barrido, Análisis Elemental y Mapeo por espectrometría de Energía Dispersiva, Análisis de Espectroscopía de Infrarrojo y Difracción de rayos X. Al realizar estos métodos de síntesis se busca obtener un material homogéneo, establecer una metodología para obtener el compósito y mejorar las propiedades fotocatalíticas.



#### Fintech, Transformation, Finance

**Citation:** Dávalos-Rosas, Vivian Guadalupe, García-González, Nidia, Enríquez-Pérez, Ma. de los Ángeles and Castrejón-Sánchez, Víctor Hugo. [2024]. Comparison of methods for obtaining a hydroxyapatite and zinc oxide composite (HAp/ZnO). Journal of Technical Invention. 8[21]-1-12: e10811112.



ISSN 2523-6792/© 2009 The Author[s]. Published by ECORFAN-Mexico, S.C. for its Holding Taiwan on behalf of Journal of Technical Invention. This is an open access article under the CC BY-NC-ND license [<http://creativecommons.org/licenses/by-nc-nd/4.0/>]

Peer Review under the responsibility of the Scientific Committee MARVID® - in contribution to the scientific, technological and innovation Peer Review Process by training Human Resources for the continuity in the Critical Analysis of International Research.

## Introduction

Currently, it is important to search different chemical routes for material synthesis, this approach allows for the development of synthetic materials using methodologies that reduce or eliminate wastes, employing environmentally friendly processes. These materials can be used in various fields, such as photocatalysis, antibacterial materials, biomedical applications, among others (Marinas A., 2007), (Doria S., 2009), (Hernández L. , M., & Prieto S., G., 2017).

Zinc oxide ( $\text{ZnO}$ ) is a semiconductor with an exciton binding energy of 60 meV and a band gap energy of 3.37 eV, emitting exclusively in the UV range and exhibiting piezoelectricity. This oxide is biocompatible, making it suitable for biomedical, antibacterial, UV protection, optoelectronic, and catalysis applications (Wen, T., Gao, J., Shen, J., y Zhou, Z., 2001).

Hydroxyapatite (HAp) is basically composed of calcium and phosphorus, although depending on the synthesis method, it may contain traces of elements such as sodium and magnesium. One of the main characteristics of this material is the calcium-phosphorus molar ratio; the lower the ratio, the higher the acidity and solubility of the samples, which is also a factor related to the mechanical properties of the material. Pure-phase HAp has a Ca/P molar ratio of 1.67 and exhibits greater stiffness compared to HAp with a different molar ratio. When the ratio is 1.5, calcium-deficient samples are obtained, and if the molar ratio is higher than 1.67, it contains carbonate groups and traces of Mg. Additionally, HAp with molar ratios ranging from 1.5 to 2.0 has been used as ceramic coatings (Enríquez P. M. A., Castrejón S. V. H., Rosales D. J., Díaz C. F. J. A., 2020), (H. Dai, T. Xinwei , H. Zhu, T. Sun y X. Wang , 2018).

It is important to highlight that in the quest to improve various materials, oxide composites with supports or coupled materials have emerged, such as reinforced rubber, mortar and concrete, alloys, porous and fractured media, fiber composites, polycrystalline aggregates (metals), heterogeneous catalysts, and so on (Campbell, 2010), (Hashin, 1983).

Zinc oxide and hydroxyapatite have been integrated into composite materials (Sowińska-Baranowska, A., & Maciejewska, M., 2024) (Gupta, R., Singh, V. P., & Agarwal, M., 2024). In 2015, Ochoa-Fajardo D.A. synthesized a zinc oxide composite impregnated in a granular support that exhibited photocatalytic activity. The photocatalytic of  $\text{ZnO}$  was taken in advantage by using two granular supports (activated carbon and andesite) and two impregnation methods (controlled precipitation and solvent evaporation) (activated carbon and andesite) and two impregnation methods (controlled precipitation and solvent evaporation) (Fajardo, 2015). In 2016, Gálvez-Co et al. developed hydroxyapatite doped with  $\text{ZnO}$  nanoparticles for potential biomedical applications. Gálvez-Coy obtained natural hydroxyapatite from bone and studied the antimicrobial activity of the samples against *Pseudomonas aeruginosa* ATCC 9027 and *Staphylococcus aureus* ATCC 25923 (Gálvez-Coy, 2016). In 2019, Charlena et al. realized the synthesis and characterization of Zinc Oxide/Hydroxyapatite to obtain an antibacterial biomaterial. The hydroxyapatite was made from Snail shells (*Bellamya javanica*) due to their high calcium content, and the  $\text{ZnO}$  was synthetized using the low-temperature hydrothermal method (Charlena, Suparto, & Kurnia, 2019).

For photocatalysis, the formation of composites has been implemented, as modifying the properties of the main compound with another material can meet specific requirements. There are many methods available for the preparation of zinc oxide composites, which are divided into hydrochemical and pyrotechnical methods (Fajardo, 2015), (Iglesias-Juez, A., Kubacka, A., Colón, G., y Fernández-García, M., 2013), (Rashtiani, M., Ghasemi, E., Hallajian, S., & Ziyadi, H., 2024) (Das, A., Ringu, T., Ghosh, S., & Pramanik, N., 2024) (El Bekkali, C., Abbadi, M., Labrag, J., Es-saidi, I., Robert, D., Nunzi, J. M., & Laghzizil, A., 2024).

Among the hydrochemical and pyrotechnical methods for composite synthesis, notable techniques include solution impregnation (Zhong, J. B., Li, J. Z., He, X. Y., Zeng, J., Lu, Y., He, J. J., y Zhong, F., 2014), controlled precipitation (Ngo, G. V., Margaillan, A., Villain, S., Leroux, C., y Bressy, C., 2013), microwave-assisted synthesis (Assi, N., Mohammadi, A., Sadr Manuchehri, Q., y Walker, R. B., 2014), hydrothermal deposition (Sahoo, T., Kim, M., Baek, J. H., Jeon, S. - R., Kim, J. S., Yu, Y. - T., ... Lee, I. -H., 2011), composite synthesis in emulsion (Lim, B. P., Wang, J., Ng, S. C., Chew, C. H., y Gan, L. M., 1998 ), mechanical mixing (Mohammadi, M., Sabbaghi, S., Sadeghi, H., Zerafat, M. M., y Pooladi, R., 2014), solvent evaporation (Shahid, M., McDonagh, A., Kim, J. H., y Shon, H. K., 2014), and physical vapor deposition (Thangadurai, P., Zergioti, I., Saranu, S., Chandrinou, C., Yang, Z., Tsoukalas, D., Boukos, N., 2011). In this work, hydroxyapatite was synthesized, zinc oxide was produced using sol-gel synthesis (Contreras-de La Cruz, M. A., García-González, N., Enríquez-Pérez, Ma. Ángeles And Castrejón-Sánchez, V. H., 2022) and electrolysis synthesis with zinc electrodes (Castrejón-Sánchez, V. H., Gacía-González, N., Enríquez-Pérez, Ma. Ángeles and Hernández-Bernardino, B., 2021), and hydroxyapatite was incorporated into the precursors of each zinc oxide synthesis.

## Methodology

### Materials

Eggshell, Hydrogen Peroxide (90%, Sigma Aldrich), Phosphoric Acid (85%, Sigma Aldrich), distilled water, zinc acetate, oxalic acid, sodium chloride.

Synthesis was carried out in two stages: in first stage, the materials were obtained separately. For second stage, the composite was prepared using sol-gel and electrolysis together. The methodology used is described below.

### HAp Synthesis

For HAp synthesis, eggshells were collected, washed, and dried. They were treated with a 30%  $H_2O_2$  solution at 95°C for 1 h, followed by washing the material with distilled water.

The material was dried at 80°C for 48 h. Subsequently, it was impregnated with 1M  $H_3PO_4$  using the methodology proposed by Enríquez (Enríquez P. M. A., Castrejón S. V. H, Rosales D. J., Díaz C. F. J. A., 2020). The material was calcined at 800°C for 2 h.

### ZnO Synthesis

#### *Sol-Gel synthesis*

Two solutions were prepared: Solution A: zinc acetate was dissolved in ethanol and heated to 60°C for 1 h. Solution B: oxalic acid was mixed in ethanol and heated to 50°C for 1 h; both solutions were stirred constantly. Solution A was added to Solution B, forming a gel, which was dried at 80°C for 20 h. Finally, the material underwent a thermal treatment at 650°C for 30 min, resulting in ZnO powders, which were labeled for characterization.

#### *Electrolysis Synthesis*

Sodium chloride was dissolved in water, and this solution was placed in an electrochemical cell, with zinc as both the anode and cathode. The solution was stirred for 30 min at 19 V and 0.33 Amp. The sample was then washed and filtered, followed by thermal treatment at 450°C for 2 h. The resulting ZnO was labeled for characterization.

### Composite Synthesis

The composite was obtained by preparing HAp as described previously and it is pour into the electrochemical cell used for ZnO synthesis and the electrochemical process is repeated. The resulting material was then washed and filtered, followed by heat treatment for 2 h at 450°C, yielding a powder of the HAp/ZnO composite, which was labeled for characterization.

#### *Sol-Gel Methodology*

Zinc acetate was mixed with ethanol, and the solution was stirred and heated to 60°C for 45 min. HAp was then added, and the mixture was stirred for 15 min. Separately, a solution of oxalic acid with ethanol was prepared and stirred for one h at 50°C. Afterward, the two solutions were combined, forming a gel that was dried at 80°C for 20 h.

Finally, the obtained material was calcined at 650°C for 1 h, resulting in a powder. The HAp/ZnO composite was labeled for characterization.

### *Electrolysis Synthesis*

Sodium chloride and HAp were dissolved in water, and the solution was stirred for 30 min. The solution was placed in an electrochemical cell, where both the anode and cathode were zinc. The electrolysis process was carried out for 30 min, with the sample under constant stirring at 19 V and 0.33 amperes.

### **Material characterization**

The characterization of HAp, ZnO, and the composites was carried out using the following techniques: X-Ray Diffraction (XRD) to determine the crystallographic planes of the material, using a Bruker DXR Discover D8 model, obtaining a diffractogram in the range from 15° to 90° range in 2θ geometry. Fourier-Transform Infrared Spectroscopy (FTIR) was used to identify the functional groups present; a Perkin Elmer UATR Two spectrophotometer was used, with spectra ranging from 4000 to 500 cm<sup>-1</sup>. Scanning Electron Microscopy (SEM) was employed to analyze the morphology of the materials and their elemental composition via Energy Dispersive Spectroscopy (EDS), using a JEOL JSM-IT100 Scanning Electron Microscope coupled with a Bruker Nano D-12489 probe, operating at 20 kV acceleration voltage, high vacuum, and secondary electron signal.

### **Results and Discussion**

In Figures 1 to 3, the micrographs of the individual components that compose the HAp/ZnO composite can be observed. The goal is to understand the effect that the synthesis process has on the morphology of each component and whether these morphologies are retained when the composite is obtained.

Figure 1 is a micrograph corresponding to HAp, which is the result of the chemical treatment with phosphoric acid and the subsequent heat treatment of calcium carbonate derived from eggshell.

The morphology of the HAp (which will serve as the composite's support) closely resembles coral, which has been previously reported ([N. Mohan, R. P. F. B. Fernandez y H. Varm, 2018](#)), ([Contreras-de La Cruz, M. A., García-González, N., Enríquez-Pérez, Ma. Ángeles And Castrejón-Sánchez, V. H., 2022](#)). According to Mohan et al. ([N. Mohan, R. P. F. B. Fernandez y H. Varm, 2018](#)), these types of porous morphologies are the result of the controlled evolution of CO<sub>2</sub> gas during the reaction between calcium carbonate and the phosphate group in the phosphoric acid solution.

### **Box 1**

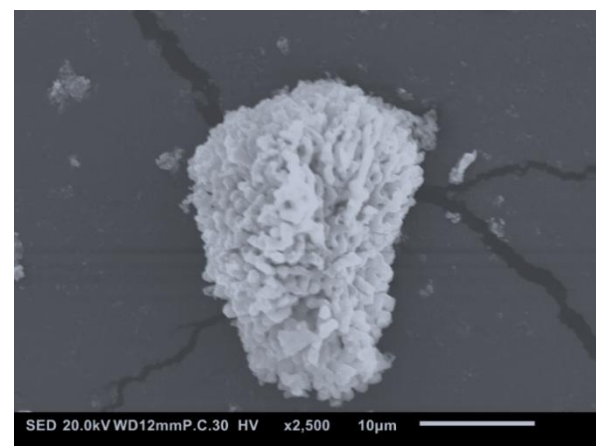


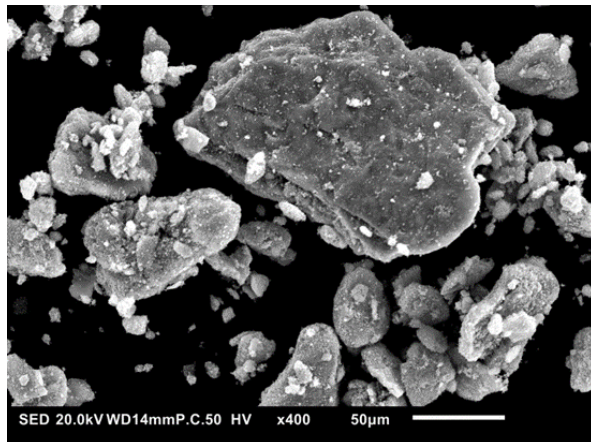
**Figure 1**

Hydroxyapatite Micrograph

*Source: own elaboration*

The sol-gel process allowed to produce a particulate material that does not exhibit a predominant morphology (Figure 2).

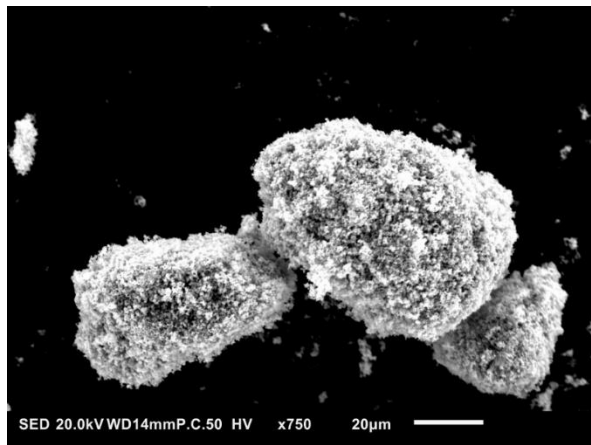
The ZnO particles show relatively flat and continuous surfaces, which may present a clear disadvantage in the photocatalysis process in which they will be used. The particle sizes obtained through this method range from 15 to approximately 175 µm.

**Box 2****Figure 2**

ZnO Sol-Gel Micrograph

Source: own elaboration

The ZnO obtained by electrolysis (Figure 3) exhibits a highly irregular surface and appears to be quite porous. This characteristic could be an advantage for ZnO, as in the photocatalytic processes where it will be used, porosity is accompanied by a larger surface area compared to a material with a continuous surface. The size of the ZnO particles ranges from 40 to 70  $\mu\text{m}$ .

**Box 3****Figure 3**

ZnO Electrolysis Micrograph

Source: own elaboration

**Elemental Analysis**

Energy Dispersive Spectroscopy (EDS) was performed to analyzed the elemental composition of the composites and individual compounds. When comparing the atomic percentages of the individual components, the ZnO synthesized by electrolysis is very similar to that obtained by sol-gel synthesis, with stoichiometries close to the 1:1 atomic ratio.

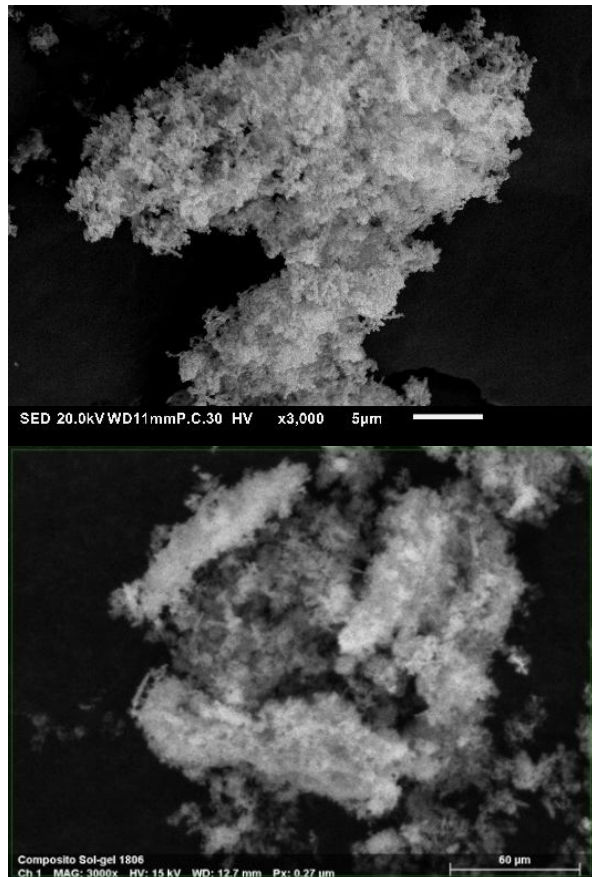
The atomic Ca/P ratio for HAp is 38.11, in the Sol-Gel composites it was 8.91, and 66.25 for Electrolysis, respectively; this ratio increases with the rise in carbonate ion content, as the  $\text{CO}_3^{2-}$  ion replaces  $\text{PO}_4^{3-}$  (Ochoa I., López E., Copete H., 2021), these ratios indicate that the hydroxyapatite is both hydroxylated and carbonated (Markovic, M., Fowler, B. O., & Tung, M. S., 2004).

Additionally, the Ca/Zn ratio in the composites was calculated, with a value of 2.38 for Sol-Gel, indicating that there are approximately two Ca atoms for each Zn atom. For Electrolysis, the ratio is 33.13, meaning there are approximately 33 Ca atoms for each Zn atom. These ratios are associated with the formation of composites (Contreras-de La Cruz, M. A., García-González, N., Enríquez-Pérez, Ma. Ángeles And Castrejón-Sánchez, V. H., 2022).

In the composites, it is observed that zinc decreases according to the type of synthesis having 3.04% At. for HAp/ZnO Sol-Gel and 0.4% At. for ZnO/HAp Electrolysis. We assume that it is because the sol-gel technique allows better incorporation between ZnO and HAp.

**Sol-Gel Composite**

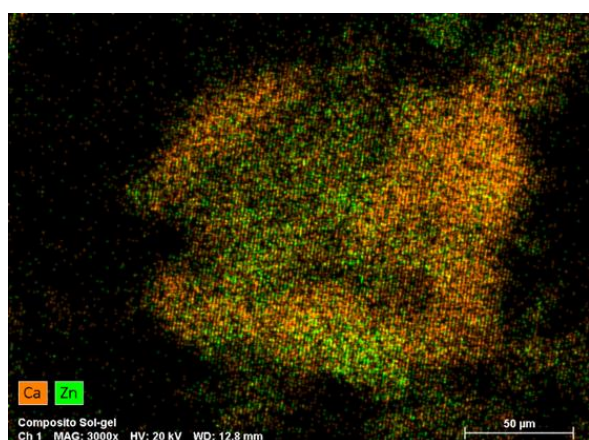
Figure 4 corresponds to the HAp composite with ZnO obtained by sol-gel. The displayed morphology for this material appears without a defined structure, differing significantly from the morphologies of the individual HAp and ZnO components (Figures 1 and 2, respectively). A surface mapping of the particle was conducted to determine the distribution of ZnO on the HAp support (Figure 5), where the green color is associated with Zn from ZnO and the orange with Ca from  $\text{CaCO}_3$ .

**Box 4****Figure 4**

HAp/ZnO Sol-Gel Micrograph

*Source: own elaboration*

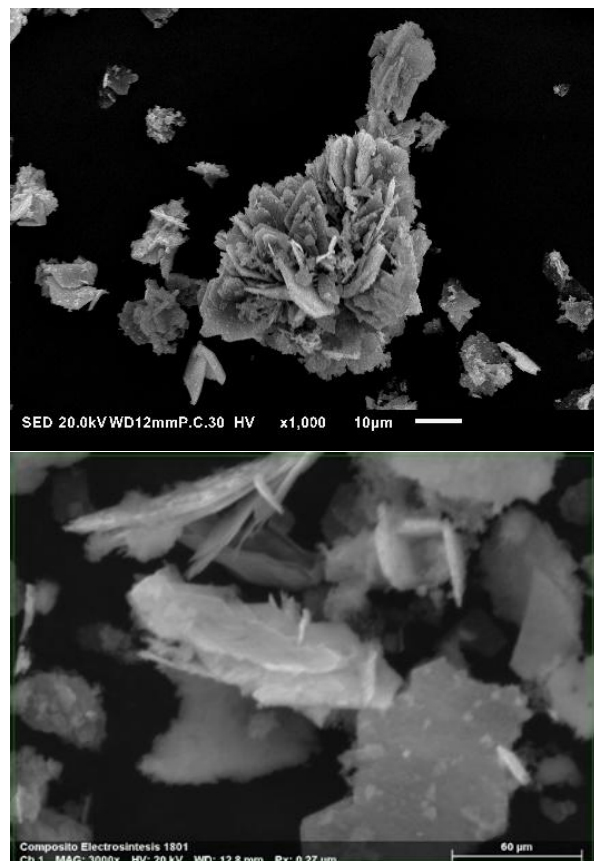
It is evident that the distribution of ZnO on the surface of  $\text{CaCO}_3$  is quite homogeneous, as shown in Figure 5. The micrograph's background was removed to make the distribution of the elements clearer.

**Box 5****Figure 5**

HAp/ZnO Sol-Gel Mapping

*Source: own elaboration**Electrosynthesis Composite*

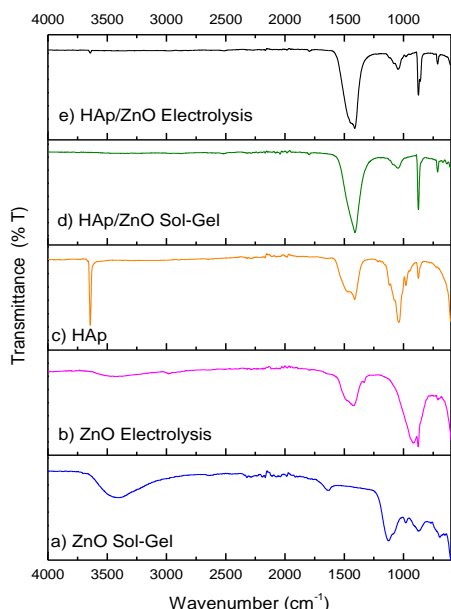
For the composite obtained through electrosynthesis, elemental mapping was also performed, like the previous composite. In the micrograph in Figure 6, the morphology of the HAp/ZnO composite can be observed. In this case, the morphology resembles flakes, which is very different from the morphology of both HAp and ZnO.

**Box 6****Figure 6**

HAp/ZnO Electrolysis Micrograph

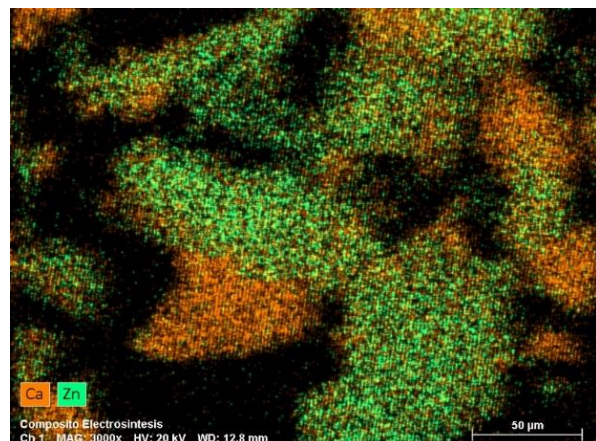
*Source: own elaboration*

Figure 7 represents the distribution of ZnO (green) on the HAp support indicated in orange, which shows that the distribution of ZnO on the surface of HAp is less homogeneous than in the previous case, as there are many areas of HAp (orange) without ZnO on its surface. To improve the visualization of the compounds' distribution, the background micrograph in Figure 7 was removed.

**Box 8****Figure 8**

Spectra of FTIR

Source: own elaboration

**Box 7****Figure 7**

HAp/ZnO Electrolysis Mapping

Source: own elaboration

**FTIR Spectroscopy**

Figure 8 shows the FTIR spectra of the samples. Both techniques confirm the formation of ZnO, with small shifts in the absorptions.

When ZnO is prepared by sol-gel, the peaks at  $3404\text{ cm}^{-1}$  and  $1651\text{ cm}^{-1}$  correspond to OH stretching vibrations and bending modes of absorbed water (Sowri, Ramachandra, Sujatha, Venugopal, & Mallika, 2013).

The vibrations at  $1131\text{ cm}^{-1}$ ,  $966\text{ cm}^{-1}$ ,  $883\text{ cm}^{-1}$ , and  $646\text{ cm}^{-1}$  are due to the tension of the Zn-O bond, indicating the formation of ZnO (Awasthi, Adhikari, Ko, Park, & Kim, 2016) (Galindo G., Fortis H., De La Rosa R., Zermeno G., & Galindo G., 2022), (Maher, S.; Nisar, S.; Muhammad A., S.; Saleem, F.; Behlil, F.; Imran, M.; Assiri, M. A.; Nouroz , A.; Naheed, N.; Khan, Z. A. ; Aslam, P., 2023).

By electrolysis (Figure 8b), the signal at  $3456\text{ cm}^{-1}$ , which corresponds to the OH bending stretch of absorbed water (Sowri, Ramachandra, Sujatha, Venugopal, & Mallika, 2013), is predominant. The Zn-O bond tension is observed at  $914\text{ cm}^{-1}$ ,  $873\text{ cm}^{-1}$ , and  $705\text{ cm}^{-1}$ , characteristic signals of ZnO formation (Faria, y otros, 2022). We assume that these shifts are due to the fact that the precursors used in this synthesis cannot be completely eliminated.

In Figure 8c, the peak at  $3632\text{ cm}^{-1}$  corresponds to the stretching of the hydroxyl group associated with the OH group of HAp. The absorption at  $1412\text{ cm}^{-1}$  is due to the presence of carbonate groups, and at  $1040\text{ cm}^{-1}$ , characteristic of phosphate groups. The signal at  $880\text{ cm}^{-1}$  is attributed to the presence of both carbonate and phosphate groups, characteristic signals of HAp (Adeogun, y otros, 2018).

The ZnO/HAp composite, regardless of the preparation technique, essentially shows the same signals with slight shifts (see Figures 8d and 8e). The presence of ZnO influences the vibrations of HAp due to steric hindrances, leading to a reduction in the vibrational energy of the HAp molecule (Molodovan M, 2015).

The intensity of the  $3632\text{ cm}^{-1}$  band decreases because of the interaction between ZnO and the OH groups of HAp (Charlena, Suparto, & Kurnia, 2019); the absorption of carbonate groups at  $1420$  and  $833\text{ cm}^{-1}$  is more intense due to the interaction between the materials (Azam A, 2012), (Molodovan M, 2015). The absorption at  $1019\text{ cm}^{-1}$ , attributed to phosphate groups, decreases because of the interaction between ZnO and  $\text{PO}_4$ , indicating that HAp is influenced by Zn (Molodovan M, 2015) (Charlena, Suparto, & Kurnia, 2019). The absorption bands of ZnO present in the material before mixing with HAp do not appear in the FTIR spectrum, except for a band at  $646\text{ cm}^{-1}$  at lower wavenumbers.

The prepared composites exhibit homogeneity, this means that ZnO and HAp are well combined (Charlena, Suparto, & Kurnia, 2019) (Azam A, 2012).

### X-ray diffraction

Figure 9 shows the results for X-Ray Diffraction analysis of the composites (HAp/ZnO Sol-Gel and ZnO/HAp Electrolysis) and the precursors HAp, ZnO Sol-Gel, and ZnO Electrolysis.

The ZnO (Figure 9a and 9b) displays 2 $\theta$  peaks at 31.9°, 34.6°, 36.4°, 47.8°, 56.8°, 68.3°, and 69.4°, with their respective diffraction planes (-100), (00-2), (-10-1), (-10-2), (-210), (-21-2), and (-20-1), respectively. These angles are characteristic of the hexagonal Wurtzite phase of ZnO previously reported (Alami, Z., Salem, M., Gaidi, M., & Elkham, J., 2015), (Baneto, M., Enesca, A., Lare, Y., Jondo, K., Napo, K., & Duta, A., 2014), (Carta de difracción COD-2300113, Sowa Heidrun, Ahsbabs Hans, 2006).

Figure 9c shows the diffractogram of HAp, with the peaks at 2 $\theta$  angles of 19.6°, 28.99°, 46.66°, 51.1°, 54.7°, and 63°, along with their respective reported diffraction planes (El hadad, A. A.; Barranco, V.; Jiménez M., A. ; Peon, E.; Galván, J. C., 2010), (Hendricks S., Jefferson M., Mosley V., 1932), (Carta de Difracción COD 1100066: Al<sub>2</sub>O<sub>3</sub>-ZrO<sub>2</sub> standar).

Since it is a carbonated HAp, it is possible that Zn ions occupy the sites corresponding to the CO<sub>3</sub><sup>2-</sup> y PO<sub>4</sub><sup>3-</sup> ions. When HAp and ZnO are coupled, the signals become broader, and the intensity increases (see Figure 9d and 9e). Contreras-de La Cruz, M. *et Al.* (Contreras-de La Cruz, M. A., García-González, N., Enríquez-Pérez, Ma. Ángeles And Castrejón-Sánchez, V. H., 2022) also confirmed that both signals shift slightly, which is also observed in the infrared spectrum (Figure 8d and 8e).

### Box 9

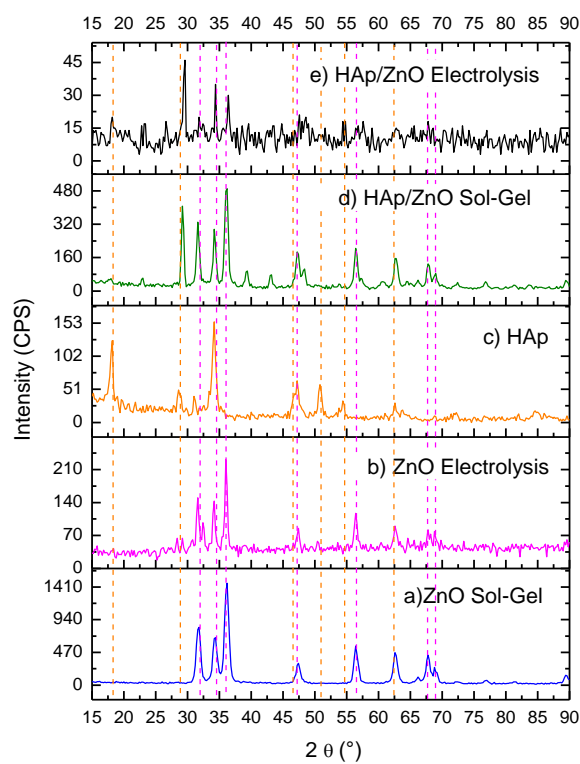


**Figure 9**

Diffractograms

Source: own elaboration

### Conclusions

The HAp/ZnO composite was obtained through two synthesis routes (Sol-Gel and Electrolysis); to achieve homogeneity, hydroxyapatite was added during the preparation of the ZnO precursor, followed by a thermal treatment.

In the scanning electron microscopy images, the influence of the synthesis method on morphology is evident. Through electrolysis, the formation of agglomerated sheets is observed, whereas in the Sol-Gel method, no defined morphology is seen, and only pores are observed, which could facilitate the photocatalytic process. The elemental analysis allowed the quantification of the atomic percentages of each composite, showing that the Zinc drastically decreases in the Electrolysis composite (0.4% At) in comparison with the Sol-Gel composite with a Zn content of 3.04% At. The mapping shows that Zn and Ca are homogeneously distributed, where Zn associated with ZnO and Ca with HAp.

Infrared spectroscopy confirmed the formation of both composites; however, it is not possible to distinguish between them.

The X-ray diffraction analysis confirmed the presence of HAp and ZnO in both composites. The crystallinity of the Electrolysis composite decreased, which may be associated with the morphological changes and the reduction in the atomic percentage of Zn.

## **Declarations**

### **Conflict of interest**

The authors declare no interest conflict. They have no known competing financial interests or personal relationships that could have appeared to influence the article reported in this article.

### **Author contribution**

*Dávalos-Rosas, V. G.:* Contributed to the synthesis of the materials studied in the article.

*García-González, N.:* Contributed to the project idea, the characterization, and the discussion of the results of the materials studied in the article.

*Enríquez-Pérez, Ma. Angeles:* Contributed to the project idea, the characterization, and the discussion of the results of the materials studied in the article.

*Castrejón-Sánchez, V.H.:* Contributed to the project idea, the characterization, and the discussion of the results of the materials studied in the article.

### **Availability of data and materials**

The synthesized materials and all the data from the analyses carried out in this research are available.

### **Funding**

We thank TecNM for the financial support through “Convocatoria 2024 Proyectos de Investigación Científica, Desarrollo Tecnológico e Innovación”.

### **Acknowledgements**

The authors thank the Academy-Industry Cooperation Center of the Tecnológico de Estudios Superiores de Jocotitlán for all the support provided through access to the XRD, FTIR, SEM and EDS equipment.

## **Abbreviations**

DXR	X-ray diffraction
EDS	Energy Dispersive Spectroscopy
FTIR	Fourier Transform Infrared Spectroscopy
HAp/ZnO Electrolysis	Composite synthesized by Electrolysis.
HAp/ZnO Sol-Gel	Composite synthesized by Sol-Gel.
HAp	Hydroxyapatite
SEM	Scanning Electron Microscopy.
ZnO	Zinc Oxide

## **References**

### *Antecedents*

Assi, N., Mohammadi, A., Sadr Manuchehri, Q., y Walker, R. B. (2014). *Synthesis and characterization of ZnO nanoparticle synthesized by a microwave-assisted combustion method and catalytic activity for the removal of ortho-nitrophenol*. *Desalination and Water Treatment*, 0(0), 1-10.

Campbell, F. C. (2010). *Structural composite materials. Chapter 1: Introduction to Composite Materials*. ASM International. , Query Date: June 2022.

Charlena, Suparto, I., & Kurnia, E. (2019). *Synthesis and Characterization of Hydroxyapatite-Zinc Oxide (HAp-ZnO) as Antibacterial Biomaterial*. *Conf. Ser.: Mater. Sci. Eng*, 1-7.

Das, A., Ringu, T., Ghosh, S., & Pramanik, N. (2024). *Polycaprolactone Microsphere Encapsulated Fluconazole-Loaded Zinc Oxide and Hydroxyapatite Nanocomposites for Enhanced Biological Performance*. *ChemistrySelect*, 9(14), e202400248,

Doria S., M. (2009). *Química verde: un nuevo enfoque para el cuidado del medio ambiente*. *Educación Química*, 412-420.

El Bekkali, C., Abbadi, M., Labrag, J., Es-saidi, I., Robert, D., Nunzi, J. M., & Laghzizil, A. (2024). *Enhancing the Photocatalytic Degradation of Selected Estrogenic Hormone Using ZnO/Hydroxyapatite Nanocomposite*. *Chemistry Africa*, 1-10.

Enríquez P. M. A., Castrejón S. V. H, Rosales D. J., Díaz C. F. J. A. (2020). *Hidroxiapatita sintetizada a partir del reciclaje de cascarón de huevo.* *Revista de Invención*, 1-6.

Fajardo, D. A. (2015). *Tesis: Desarrollo de un material compósito de ZnO Impregnado en un soporte granular que presente actividad fotocatalítica.* Quito: Escuela Politecnica Nacional.

Gálvez-Coy, D. (2016). *Tesis de Maestría: Obtención y caracterización de Hidroxiapatita dopada con nanoparticulas de ZnO con potenciales aplicaciones biomédicas.* Colombia: Universidad Nacional de Colombia Facultad de Ciencias Exactas y Naturales, Departamento de Física y Química Manizales.

Gupta, R., Singh, V. P., & Agarwal, M. (2024). Metallurgical and interfacial co-relation of HA ZnO-Fe3O4 composite for implant application with properties: experimental interaction study with ANOVA and ANCOVA model. *Phase Transitions*, 97(4-5), 322-336.

H. Dai, T. Xinwei , H. Zhu, T. Sun y X. Wang . (2018). Effects of Commonly Occurring Metal Ions on Hydroxyapatite Crystallization for Phosphorus Recovery from Wastewater . *Water*, 1-12.

Hashin, Z. (1983). Analysis of Composite Materials- A Survey. *Journal of Applied Mechanics. Query Date: 16/05/2022*, 482-505.

Hernández L. , M., & Prieto S., G. (2017). El papel de la fotocatálisis en la protección ambiental y la química verde. *Recopilación - Química - Investigación Joven*, 4(1), 40-44.

Iglesias-Juez, A., Kubacka, A., Colón, G., y Fernández-García, M. (2013). *Chapter 10 - Photocatalytic Nanooxides: The Case of TiO<sub>2</sub> and ZnO.* In S. L. Suib, pp. 245-266. Amsterdam: Elsevier: New and Future Developments in Catalysis.

Lim, B. P., Wang, J., Ng, S. C., Chew, C. H., y Gan, L. M. (1998). A Bicontinuous Microemulsion Route to Zinc Oxide Powder. *Ceramics International*, 24(3), 205-209.

Marinas A., A. (2007). *Catálisis heterogénea y química Verde . An. Quím. ISSN-e 2792-5250, ISSN 1575-3417*, 103(1), 30–37.

Mohammadi, M., Sabbaghi, S., Sadeghi, H., Zerafat, M. M., y Pooladi, R. (2014). Preparation and characterization of TiO<sub>2</sub>/ZnO/CuO nanocomposite and application for phenol removal from wastewaters. *Desalination and Water Treatment*, 0(0), 1-11.

Ngo, G. V., Margaillan, A., Villain, S., Leroux, C., y Bressy, C. . (2013). Synthesis of ZnO nanoparticles with tunable size and Surface hydroxylation. *Journal of Nanoparticle Research*, 15(1), 1-15.

Rashtiani, M., Ghasemi, E., Hallajian, S., & Ziyadi, H. (2024). Green synthesis of nanocomposite based on magnetic hydroxyapatite using *Falcaria vulgaris* Bernh leaf extract to remove tartrazine dye from aqueous solution. *Inorganic Chemistry Communications*, 163, 112361.

Sahoo, T., Kim, M., Baek, J. H., Jeon, S .- R., Kim, J. S., Yu, Y .- T., ... Lee, I .-H. (2011). Synthesis and characterization of porous ZnO nanoparticles by hydrothermal treatment of as pure aqueous precursor. *Materials Research Bulletin*, 46(4), 525-530.

Shahid, M., McDonagh, A., Kim, J. H., y Shon, H. K. (2014). Magnetised titanium dioxide (TiO<sub>2</sub>) for water purification: preparation, characterisation and application. *Desalination and Water Treatment*, 0(0),1-24.

Sowińska-Baranowska, A., & Maciejewska, M. (2024). Effect of dispersants on the hydroxyapatite-filled natural rubber biocomposites with enhanced functional properties. *Journal of Applied Polymer Science*, 141(20), e55367.

Thangadurai, P., Zergioti, I., Saranu, S., Chandrinou, C., Yang, Z., Tsoukalas, D., Boukos, N. (2011). ZnO nanoparticles produced by novel reactive physical deposition process. *Applied Surface Science*, 257(12), 5366-5369. <http://doi.org/10.1016/j.apsusc.2010.12.001>.

Wen, T., Gao, J., Shen, J., y Zhou, Z. ( 2001). Preparation and characterization of TiO<sub>2</sub> thin films by the sol-gel process. *Journal of Materials Science*, 36(24), 5923-5926.

Zhong, J. B., Li, J. Z., He, X. Y., Zeng, J., Lu, Y., He, J. J., y Zhong, F. (2014). Fabrication and Catalytic Performance of SiO<sub>2</sub>-ZnO Composite Photocatalyst. *Synthesis and Reactivity in Inorganic, Metal-Organic, and Nano-Metal Chemistry*, 44(8),1203-1207.

#### *Basics*

Castrejón-Sánchez, V. H., Gacía-González, N., Enríquez-Pérez, Ma. Ángeles and Hernández-Bernardino, B. (2021). Preparation advances of Activated-Carbon/ZnO composite using ground coffee. *Journal of Chemical and Physical Energy*, 8-24:8-14.

Contreras-de La Cruz, M. A., García-González, N., Enríquez-Pérez, Ma. Ángeles And Castrejón-Sánchez, V. H. (2022). Preparation advances of hydroxyapatite/ZnO composite using egg-shell. *Journal of Chemical and Physical Energy*, Vol.9 No.26 8-16, DOI: 10.35429/JCPE.2022.26.9.8. 16.

Enríquez P. M. A., Castrejón S. V. H, Rosales D. J., Díaz C. F. J. A. (2020). Hidroxiapatita sintetizada a partir del reciclaje de cascaron de huevo. *Revista de Invención*, 1-6.

#### *Supports*

Contreras-de La Cruz, M. A., García-González, N., Enríquez-Pérez, Ma. Ángeles And Castrejón-Sánchez, V. H. (2022). Preparation advances of hydroxyapatite/ZnO composite using egg-shell. *Journal of Chemical and Physical Energy*, Vol.9 No.26 8-16, DOI: 10.35429/JCPE.2022.26.9.8. 16.

Enríquez P. M. A., Castrejón S. V. H, Rosales D. J., Díaz C. F. J. A. (2020). Hidroxiapatita sintetizada a partir del reciclaje de cascaron de huevo. *Revista de Invención*, 1-6.

Markovic, M., Fowler, B. O., & Tung, M. S. (2004). Preparation and Comprehensive Characterization of a Calcium Hydroxyapatite Reference Material. *Journal of Research of the National Institute of Standards and Technology*, 109(6):553-568. DOI: 10.6028/jres.109.042.

N. Mohan, R. P. F. B. Fernandez y H. Varm. (2018). Preparation of hydroxyapatite porous scaffold from a ‘coral-like’ synthetic inorganic precursor for use as a bone substitute and a drug delivery vehicle. *Materials Science and Engineering C*, vol. 92, pp. 329-337. <https://doi.org/10.1016/j.msec.2018.06.064>.

Ochoa I.,López E., Copete H. (2021). Síntesis y caracterización de polvos de hidroxiapatita carbonatada tipo b con diferentes contenidos de carbonato. *Revista Colombiana de Materiales*, pp.22-32.

#### *Discussions*

Adeogun, A., Ofudje, E., Idowu, M., Kareem, S., Vahidhabanu, S., & Babu, B. (2018). Biowaste-Derived Hydroxyapatite for Effective Removal of Reactive Yellow 4 Dye: Equilibrium, Kinetic, and Thermodynamic Studies. *ACS Omega*, 1991–2000. doi:10.1021/acsomega.7b01768

Alami, Z., Salem, M., Gaidi, M., & Elkham, J. (2015). Effect of Zn concentration on structural and optical proprieties of ZnO thin films deposited by spray pyrolysis. *Advanced Energy: An International Journal*. DOI:10.5121/aeij.2015.2402, 11-24. Query Date: June 2022.

Awasthi, G., Adhikari, S., Ko, S., Park, S., & Kim, C. (2016). Facile synthesis of ZnO flowers modified graphene like MoS<sub>2</sub> sheets for enhanced visible-light-driven photocatalytic activity and antibacterial properties. *Journal of Alloys and Compounds*, 2008-2015. doi:<https://doi.org/10.1016/j.jallcom.2016.04.267>

Azam A, A. A. (2012). Antimicrobial activity of metal oxide nanoparticles against gram-positive and gram-negative bacteria:a comparative study. *International Journal of Nanomedicine*, 6003-6009. doi:10.2147/IJN.S35347

Baneto, M., Enesca, A., Lare, Y., Jondo, K., Napo, K., & Duta, A. (2014). Effect of precursor concentration on structural, morphological and opto-electric properties of ZnO thin films prepared by International spray pyrolysis. *Ceramics*. DOI: <https://doi.org/10.1016/j.ceramint.2014.01.048.8397-8404>. Query Date: June 2022.

Carta de difracción COD-2300113, Sowa Heidrun, Ahsbahs Hans. (2006). **High-pressure X-ray investigation of zincite ZnO single crystals using diamond anvils with an improved shape.** *Journal of Applied Crystallography*, 39(2), 169-175.  
[https://doi.org/10.1107/S0021889805042457.](https://doi.org/10.1107/S0021889805042457)

(n.d.). *Carta de Difracción COD 1100066: Al<sub>2</sub>O<sub>3</sub>-ZrO<sub>2</sub> standar.*

Charlena, Suparto, I., & Kurnia, E. (2019). **Synthesis and Characterization of Hydroxyapatite-Zinc Oxide (HAp-ZnO) as Antibacterial Biomaterial.** *Conf. Ser.: Mater. Sci. Eng*, 1-7. doi:doi:10.1088/1757-899X/599/1/012011

Contreras-de La Cruz, M. A., García-González, N., Enríquez-Pérez, Ma. Ángeles And Castrejón-Sánchez, V. H. (2022). **Preparation advances of hydroxyapatite/ZnO composite using egg-shell.** *Journal of Chemical and Physical Energy*, Vol.9 No.26 8-16, DOI: 10.35429/JCPE.2022.26.9.8. 16.

El hadad, A. A.; Barranco, V.; Jiménez M., A. ; Peon, E.; Galván, J. C. (2010). **Multifunctional sol-gel derived thin film based on nanocrystalline hydroxyapatite powders.** *Journal of Physics: Conference Series*, DOI:10.1088/1742-6596/252/1/012007. 1-8. Query Date: June 2024.

Faria, F., Ruellas, T., Roveri, C., Malafatt, J., Pari, E., Giraldo, T., & Maestrelli, S. (2022). **Obtaining Porous Zinc Oxide Ceramics Using Replica Technique: Application in Photocatalysis.** *Materials Research*, 1-12. doi:<https://doi.org/10.1590/1980-5373-MR-2021-0083>

Galindo G., M., Fortis H., M., De La Rosa R., C., Zermeño G., H., & Galindo G., M. (2022). **Síntesis química de nanopartículas de óxido de zinc y su evaluación en plántulas de Lactuca sativa.** *Revista mexicana de ciencias agrícolas*, 299-308.  
 doi:<https://doi.org/10.29312/remexca.v13i28.3284>

Hendricks S., Jefferson M., Mosley V. (1932). **Carta de Difracción COD 9014313: The Crystal Structures of Some Natural and Synthetic Apatite-Like Substances \_cod\_database\_code 1011242.** *Zeitschrift fur Kristallographie*, 81, 352-369. DOI:10.1524/zkri.1932.81.1.352.

Maher, S.; Nisar, S.; Muhammad A., S.; Saleem, F.; Behlil, F.; Imran, M.; Assiri, M. A.; Nouroz , A.; Naheed, N.; Khan, Z. A. ; Aslam, P. (2023). **Synthesis and Characterization of ZnO Nanoparticles Derived from Biomass (Sisymbrium Irio) and Assessment of Potential Anticancer Activity.** *ACS Omega*, 15920-15931. doi:10.1021/acsomega.2c07621

Molodovan M, P. D. (2015). **Structural and morphological properties of HA-ZnO powders prepared for biomaterials.** *Open Chemistry*, 725-733.

Sowri, K. B., Ramachandra, A. R., Sujatha, C., Venugopal, K. R., & Mallika, A. N. (2013). **Synthesis and optical characterization of porous ZnO.** *Journal of Advanced Ceramics*, 260–265. doi:10.1007/s40145-013-0069-6.